Chapter 3
Silk-Based Materials and Composites: Fabrication and Biomedical Applications

Golnaz Najaf Tomaraei, Se Youn Cho, Moataz Abdulhafez, and Mostafa Bedewy

3.1 Introduction

Silk is a fibrous protein-based material that is produced by over 40,000 species, including arthropods and insects such as silkworms, spiders, scorpions, mites, and bees. Among the diverse variety of silks, domesticated *Bombyx mori* (*B. mori*) silkworm silk is the most abundant natural silk and historically was used for high-quality clothing due to its superior textile properties such as lightness, fineness, pleasant feel, and unique luster [1]. Over the past several decades, silk has been of great interest to the scientific community from two main perspectives: (1) its exceptional mechanical properties and (2) its excellent biological characteristics. Mechanically, the toughness of silk is comparable with any of the best synthetic high-performance materials, including Kevlar, nylon, and high-tensile steel, as summarized in Table 3.1. From a biological standpoint, silk shows excellent biodegradability, biocompatibility, and nontoxicity [3]. Therefore, considerable effort has

G. Najaf Tomaraei · M. Abdulhafez
Department of Industrial Engineering, University of Pittsburgh, Pittsburgh, PA, USA
e-mail: gon2@pitt.edu; mma89@pitt.edu

S. Y. Cho
Carbon Composite Materials Research Center, Korea Institute of Science and Technology, Jeonbuk, South Korea
e-mail: seyoucho@kist.re.kr

M. Bedewy (✉)
Department of Industrial Engineering, University of Pittsburgh, Pittsburgh, PA, USA

Department of Chemical and Petroleum Engineering, University of Pittsburgh, Pittsburgh, PA, USA

Department of Mechanical Engineering and Materials Science, University of Pittsburgh, Pittsburgh, PA, USA
e-mail: mbedewy@pitt.edu

P. J. Bártolo, B. Bidanda (eds.), *Bio-Materials and Prototyping Applications in Medicine*, https://doi.org/10.1007/978-3-030-35876-1_3

Table 3.1 Comparison of mechanical properties for silk fibers and man-made fibers [2]

Material	Strength (GPa)	Toughness (Mj/m^3)	Extensibility
B. mori silkworm silk fiber	0.6	70	0.18
Nylon	0.95	80	0.18
Kevlar	3.6	50	0.027
High-tensile steel	1.5	6	0.008

been directed toward insights into structure, processing of silk [4–7], and reproducing the properties of natural silk fiber by reconstitution or recombination [8–10].

In recent years, the rapid evolution of technology and the increase of concern over environmental issues have opened new opportunities for silk-based materials in various research fields. Many researchers have employed silk as a promising candidate material for bio-applications such as tissue engineering and drug delivery because of the facile processes to prepare various silk-based material formats, including hydrogels, films, scaffolds, and fibers, while maintaining their excellent biological properties such as biodegradability, biocompatibility, and nontoxicity [3]. Additionally, silk-derived materials such as silk-based composites have also gained considerable attention as they enable the derivation of materials with more functionalities.

This chapter begins with a general overview of the structure and properties of silk protein obtained from *B. mori* silkworm. Next, we highlight some of the methodologies used in preparation of silk-based materials with tunable secondary structure. Then, some of the biomedical applications of silk in various material formats are reviewed. In the following section, we focus on recent attempts to design silk-derived materials in various material formats for potential biomedical applications.

3.2 *Bombyx mori* Silkworm Silk: Structure, Properties, and Processing

3.2.1 Structure and Properties

As shown in Fig. 3.1, native *B. mori* silk cocoon fibers are about 10–25 μm in diameter and are composed of two types of protein: two fibrils of micro-fibrous protein, silk fibroin (SF), and a glue-like protein, sericin, which holds the core microfilaments together and accounts for ~25 wt% of the total silkworm cocoon [1]. Also, raw silk fibers contain some natural impurities such as fat, waxes, inorganic salts, and coloring matters. SF can be extracted by removing sericin and impurities through a process called degumming. It involves boiling SF in an alkaline solution.

SF from *B. mori* is composed of three distinct proteins, light chain, heavy chain, and P25, which are present in a 6:6:1 ratio. The heavy chain and the light chain are linked together by a single disulfide bond [12, 13]. There are no repetitive sequences in both P25 and light chain; they consist of 220 and 244 hydrophilic amino acids (M_w ~ 25 and 26 kDa) respectively, reflecting no associations with secondary structure of SF [14, 15]. The heavy chain is composed of 5362 amino acids (M_w ~390 kDa)

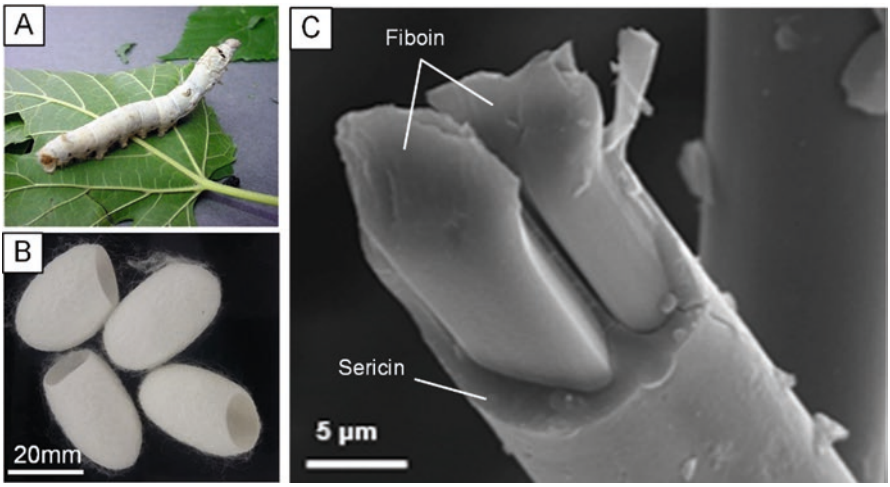

Fig. 3.1 (**a**) *B. mori* silkworm and (**b**) its cocoon fiber that consists of two fibrils of silk fibroin and a coating of sericin (**c**) as revealed by FESEM. (Reproduced from (**c**) Cho et al. [11])

mainly glycine, alanine, and serine, with a total content of above 80% [16]. The high content of these components leads to the formation of highly conserved amino acid repeat units, including GAGAGS (S is serine), GAGAGY (Y is tyrosine), GAGAGA, or GAGYGA. This promotes the construction of β-sheet crystal conformations through interchain hydrogen bonds between adjacent protein chains [17]. The amorphous regions of the heavy chain are ~40 amino acid residues in length with nonrepetitive sequence composed of charged amino acids [18, 19].

Inherently, the protein chain linked by peptide bonding is flexible to form diverse molecular conformations. However, supramolecular interactions (such as hydrogen bonding, π-interactions between aromatic groups and Van der Waals forces) result in the local conformation of polypeptide structures (secondary structure) such as α-helices, β-sheets, and turns.

Interchain hydrogen bonds between the hydrogen atom linked to the nitrogen atom and the carbonyl oxygen atom on the amino-terminal side encourage the formation of a globular structure, α-helix structure. The β-sheet conformation is organized by numerous assemblies of intra−/interchain hydrogen bonds between adjacent peptide blocks. Another secondary structure, turns, consists of four amino acids. The carbonyl oxygen of the first amino acid and the hydrogen linked to the nitrogen of the fourth amino acid form hydrogen bonding. The highly conserved primary sequence in native SF fibers determines the β-sheet-dominant secondary structure. The GX repeating units of the amino acid sequence in the crystalline domain form hydrogen bonds with each other and develop into two-dimensional chain folding, antiparallel β-sheet conformation. In addition, amino acids with small side chains such as glycine and alanine allow for inter-sheet stacking into three-dimensional nano-crystals by Van der Waals forces [2]. A typical β-sheet crystallite in SF is known to be orthogonal with the coordinate system defined with x-axis along the amino acid side chains, y-axis in the direction of the hydrogen bonds, and z-axis along the peptide bonds and with lattice constants of $a = 0.938$ nm,

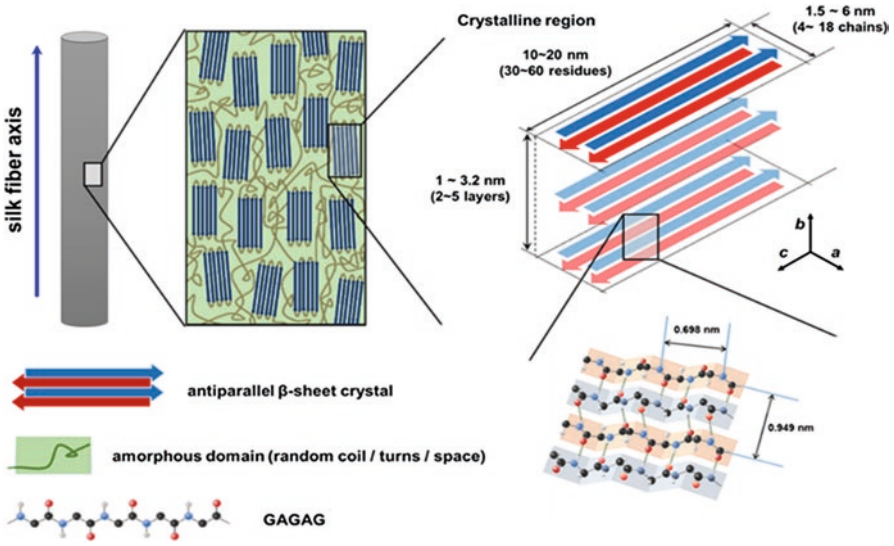

Fig. 3.2 Schematic of the hierarchical structure of β-sheet-rich silk fibroin fiber. Silk fibril shows a hetero-composite structure of stiff β-sheet crystals embedded in a soft semi-amorphous region and space. The antiparallel β-sheet crystal depicted by the ball-and-stick model (hydrogen, carbon, oxygen, and nitrogen atoms are shown as white, black, red, and blue balls, respectively). Side chains that extended above or below the sheets and alternated along the axis have been omitted for clarity

$b = 0.949$ nm, and $c = 0.698$ nm [20]. As mentioned earlier, the amorphous regions in SF are composed of non-repeated and hydrophilic amino acids. The hydrophilic amino acids are capable of hydrogen bonding with each other or with free water molecules, which enhances the flexibility of SF by acting as a plasticizer. Thus, the microstructure of native SF fibers resembles a block copolymer structure with stiff antiparallel β-sheet blocks aligned with the fiber axis and dispersed in soft amorphous segments and empty spaces as shown in Fig. 3.2. This microstructure leads to the exceptional strength while maintaining flexibility.

The β-sheet-rich structure of SF resulted from the highly conserved protein sequences results in the superior mechanical, chemical, and thermal properties of native silk fiber. Thermal and mechanical properties of SF are highly affected by absorbed water molecules below 100 °C, the boiling point of water in atmospheric pressure. In general, native silk fibers contain around 5 wt.% of water without any humidity treatment, and the absorbed water molecules are known to interact with the disordered structural components and influence the secondary structure of silk protein by acting as a plasticizer [21, 22]. The tensile strength of single fibroin fibril (prepared by degumming process) and cocoon fiber (two fibrils with sericin) shows high values in a range from 500 to 690 MPa similar to the strength of steel [23, 24]. Also, native silk fiber exhibits an excellent combination of elasticity and elongation owing to the semicrystalline structure organized by stiff β-sheets embedded in a soft semi-amorphous region. At higher temperatures above 100 °C, thermal properties of SF depend on their own chemical structure and morphologies. The onset of thermal degradation of native SF is known to be about 250 °C, which is related to the

Table 3.2 Properties of *B. mori* silkworm silk

Property		Literature
Tensile modulus (single silk fiber with sericin, GPa)	5–12	[24]
Tensile modulus (single fibril without sericin, GPa)	15–17	[23]
Tensile strength (single silk fiber with sericin, MPa)	500	[24]
Tensile strength (single fibril without sericin, MPa)	610–690	[23]
Extensibility (single silk fiber with sericin, %)	5–12	[24]
Extensibility (single fibril without sericin, %)	4–16	[23]
Glass transition temperature (°C)	178	[25]
Thermal degradation (°C)	250	[26]
Density (g/cm^3)	1.3–1.8	[27]
Crystallinity (sheet content, %)	28–62	[27]
Moisture absorption (%)	5–35	[27]

activation energy for fission of the covalent bonds in the protein's main chains [23]. The crystal melting of SF is not observed even at temperatures as high as the onset of main-chain degradation. The glass transition temperature of silk is reported around 178 °C, at which thermal and mechanical properties change dramatically [23]. In the amorphous regions, the mobility of protein chains increases prior to recrystallization, and therefore the modulus increases with temperature up to ~202 °C (Table 3.2).

Natural silkworm silk fibers possess high environmental stability due to their high crystallinity, extensive hydrogen bonds, and hydrophobic nature. As-spun silkworm silk fiber is a composite fiber of SF fibrils and sericin. On the one hand, sericin mainly consists of polar and charged amino acids and has hydrophilic properties. Thereby it's easily removed by using mild aqueous solutions under heating conditions. On the other hand, SF contains a high content of nonpolar amino acids and is insoluble in common solvents, including most alcohols and alkaline solutions, and shows only a low swelling ratio in water and dilute acids. Even strong acids such as hydrochloric acid require several hours for partial hydrolysis of SF in the amorphous regions. Also, SF shows good biodegradability and biocompatibility. Silk fiber containing highly crystallized and oriented β-sheet structure degrades slowly; however, it is possible to mediate degradation by using enzymes or controlling the content and organization of β-sheet nanocrystals [28]. As a biomaterial, SF shows good bioactive properties with similar or lower inflammatory responses compared with other biocompatible materials such as collagen and poly (lactic acid) (PLA). This was confirmed by in vitro and in vivo evaluations [29, 30].

3.2.2 Processing of SF

Natural silkworm silk fibers require straightforward processing for the textile industry such as dyeing and chemical modification to render colors and waterproofing properties, respectively [3]. However, to fit in a wide range of applications, it is

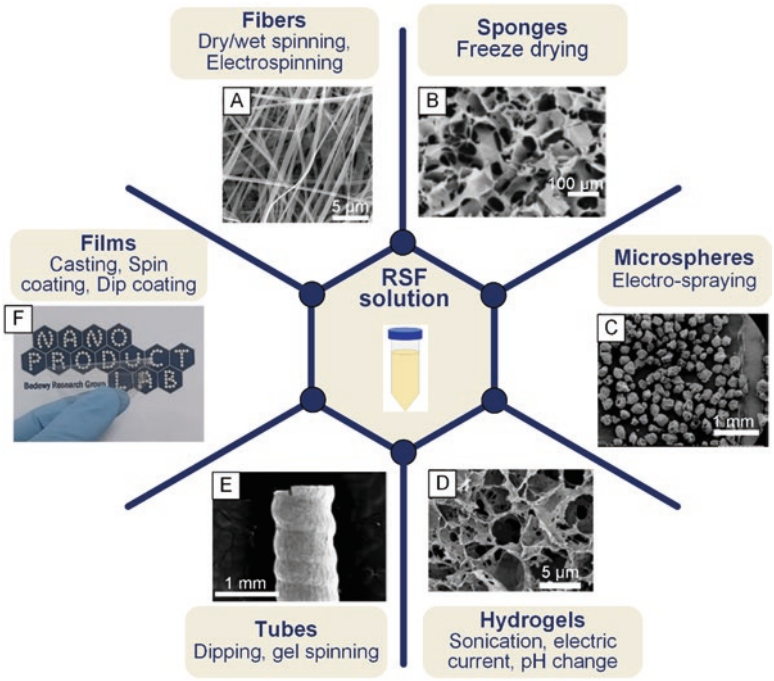

Fig. 3.3 Images of representative examples of various silk material formats and their processing methods starting from regenerated silk fibroin (RSF) solution obtained from *B. mori* silkworm silk. (**a**) Fibers, (**b**) sponges, (**c**) microspheres/microparticles, (**d**) hydrogels, (**e**) tubes, and (F) films. (Reproduced from (**a**) Sasithorn and Martinová [31]; (**b**) Tamada [32]; (**c**) Qu et al. [33]; (**d**) Kim et al. [34]; (**e**) Lovett et al. [35])

necessary to dissolve silk proteins in suitable solvents as a prerequisite step to prepare alternative material forms such as films, foams, tubes, hydrogels, fibers, and spheres as shown in Fig. 3.3. Generally, in order to break the strong intermolecular interactions between β-sheets and β-stacks in silk, concentrated aqueous solutions of inorganic/organic salts, fluorinated solvents, ionic liquids, or strong acids have been used [1, 2, 28]. Various methods have been employed to process silk into diverse material forms using regenerated SF (RSF) solution. Dry−/wet-spinning and electrospinning have been employed to create RSF fibers with micro- and nanoscale diameters, respectively. Casting, dip−/spin coating, and vacuum filtration are used to prepare RSF films. Electro-spraying and phase separation are common methods to produce RSF microspheres. Freeze-drying, gas foaming, or salt-leaching can be adjusted to prepare RSF sponges [2].

The harsh conditions during dissolving SF cause the breakage of peptide bonds in the main chain, resulting in the low crystallinity of RSF. This in turn results in inferior mechanical properties (such as brittleness and lower strength) of processed materials compared with natural SF fibers that contain high content and alignment of β-sheet crystals [36]. However, the mechanical properties of processed RSF materials can be improved by controlling the secondary structure of silk protein. This can be achieved by various treatments, which can be classified based on the processing

Table 3.3 Various treatments to tune the secondary structure of silk fibroin films

Treatment	Processing stage	Dominant resulting secondary structure	Notes	References
Formic acid dissolution	Solvent treatment	β-sheet	Requires two steps of dissolution and film casting	[38]
1,1,1,3,3,3-hexafluoroisopropyl alcohol	Solvent treatment	α-helix	Risk of chemical residues for biological application	[39]
Glycerol	Solvent treatment	α-helix	Glycerol can be totally dissolved in water	[40]
Room temp. drying	During casting	α-helix	Drying time more than 48 hrs	[41]
Casting with controlled temp. in oven	During casting	β-sheet	Slow drying in oven is needed	[42]
Water annealing	Post-processing of films	α-helix	High conc. of sol. (8 wt%) and thick film (100–200 μm) is required to have water-insoluble films	[43]
Temp. controlled water vapor treatment	Post-processing of films	Temp. dependent β content	High reproducibility Requires vacuum, Requires 12 hrs of treatment	[44]
Methanol treatment	Post-processing of films	β-sheet	Fast (10 min to 1 hour)	[38, 41]
Controlled heating	Post-processing of films	β-sheet	Transition to β-sheet starts at 140 °C	[39]

stage during which they are applied, namely, solvent treatment, treatment during processing, and post-processing treatment. For instance, post-processing exposure of silk materials to alcohols or some aqueous solutions with salts induces β-sheet formation in the materials, which enhances the mechanical properties and the stability in solvents or other environments [28, 37]. Table 3.3 summarizes some of the different treatments that have been attempted to control the secondary structure of RSF films.

3.2.3 Biomedical Applications of SF in Various Material Formats

Owing to its appealing properties such as high strength and toughness, good biocompatibility, tunable biodegradability, and permeability for oxygen and water vapor, SF in various formats is considered a potential candidate for several biomedi-

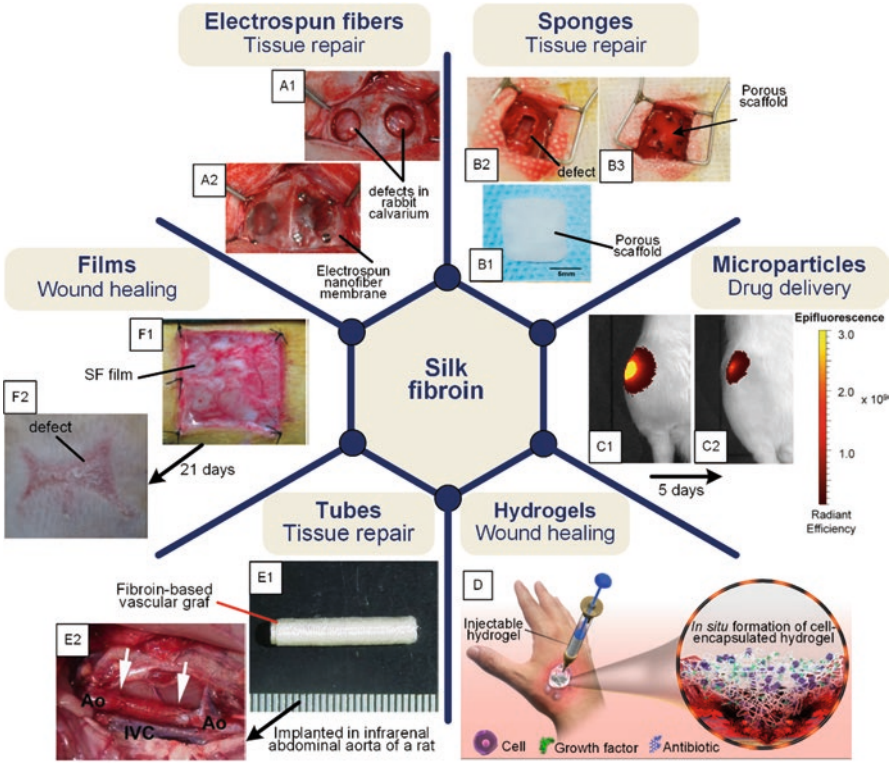

Fig. 3.4 Examples of some biomedical applications of various silk fibroin material formats. (**A1**) Defects were drilled in a rabbit calvarium model and (**A2**) the efficacy of electrospun silk membranes were evaluated in vivo. (**B1**) A porous silk fibroin scaffold to repair (**B2, 3**) a defect in the trachea of a rabbit model. (**C1**) Silk fibroin was labeled by CY7 dye as a model drug and was injected into the knee joints of rats. (C2) Persistent fluorescent after 5 days suggested slow and sustained release of the model drug. (**D**) Schematic representation of an injectable silk fibroin hydrogel that contains cells, antibiotics, and growth factor for wound healing. (**E1**) A vascular graft (**E2**) implanted inside the abdominal aorta of a rat showed blood flow without aneurysmal bulging of the graft for 1 year of study. (**F1**) Full-thickness skin defect in a rabbit model was covered with silk fibroin film, and (**F2**) defect evaluated 21 days afterwards. (Reproduced from (**A1, 2**) Kim et al. [45]; (**B1–3**) Chen et al. [46]; (**C1, 2**) Mwangi et al. [47]; (**D**) Farokhi et al. [48]; (**E1, E2**) Enomoto et al. [49]; (**F1, F2**) Zhang et al. [50])

cal applications. While in vitro cell culture studies are important to understand the behavior of SF materials in terms of cell growth and proliferation, long-term cell viability and tissue development also impact the applicability of silk-based materials in biomedical applications. Figure 3.4 illustrates representative examples of studies on in vivo behavior of various SF material forms for successful tissue reconstruction, wound healing, and small-molecule drug delivery.

3.3 Silk-Derived Materials and Composites

SF with remarkable features such as biocompatibility, tunable degradability, ease of functionalization and chemical modification, and ease of processing into various material formats has led to substantial growth in the number of studies on using SF-based materials in biomedical applications such as tissue engineering, drug delivery, and wearable implants. As mentioned earlier, while the dissolution process to prepare RSF solution makes it more versatile, it results in inferior mechanical properties. Incorporating a reinforcing agent to create SF-based composites with improved mechanical properties is a widely used approach. In addition to enhancing mechanical performance, other properties such as optical, electronic, and biological properties can also change, depending on the type of the reinforcing material. Additionally, newfound processing methods to develop novel materials have attracted considerable attention in silk research area. Among these methods are growing and assembling silk nanofibrils from RSF solution as well as SF carbonization.

The outline of this section is represented in Fig. 3.5. Here, we review studies on SF-based composites in various formats, including composite hydrogels (Fig. 3.5a), composite fibers (Fig. 3.5b), and composite films (Fig. 3.5f). We then review some of the studies on the role of SF as the reinforcing fiber (Fig. 3.5c). Hybrid nanocomposites are introduced next (Fig. 3.5d). Finally, we discuss some recent findings on carbonized silk and its application as flexible and wearable biosensors (Fig. 3.5e).

3.3.1 Composite Hydrogels

Hydrogels formed from a variety of natural polymers such as collagen and chitosan have been considered as potential biomaterials for tissue engineering. Particularly, intervertebral disk as well as cartilage tissue engineering have been major areas of focus due to the limited self-regeneration capacity of these tissues [53, 55]. As the favored scaffold format for tissue engineering, hydrogels have led to considerable progress in this area. The mechanical properties of natural hydrogels for tissue repair, however, must be improved so that they can withstand physiological loadings [55].

As a promising material for tissue repair, SF composite hydrogels have gained attention. Apart from enhancing the mechanical properties of SF hydrogels, other properties can also be improved in composite hydrogels. For instance, Ding et al. [51] noticed that adding hydroxyapatite to SF hydrogel improved the in vitro cytocompatibility and in vivo bone regeneration. Figure 3.6 shows that incorporating 60% hydroxyapatite nanoparticles in a SF hydrogel enhanced the rate of in vivo bone reconstruction when injected into model bone defects of rats.

As another example, incorporating conductive fillers such as metallic nanoparticles has been attempted to introduce interesting functionalities in silk protein.

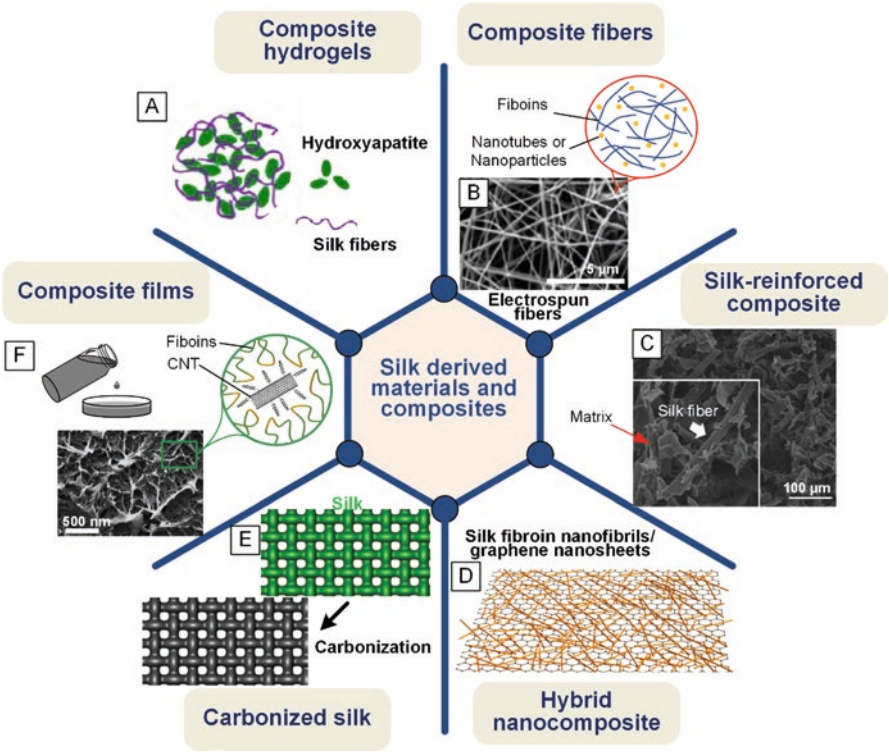

Fig. 3.5 Representative examples of silk-derived materials, including silk-based composites in various formats, that is, (**a**) hydrogels, (**b**) fibers, (**f**) films, (**c**) silk-fiber-reinforced composites, (**d**) nanohybrids containing silk fibroin nanofibrils and (**e**) carbonized silk. (Reproduced from (**a**) Ding et al. [51]; (**b**) Pan et al. [52]; (**c**) Yodmuang et al. [53]; (**d**) Ling et al. [77]; (**e**) Wang et al. [54]; and (**f**) Cho et al. [17])

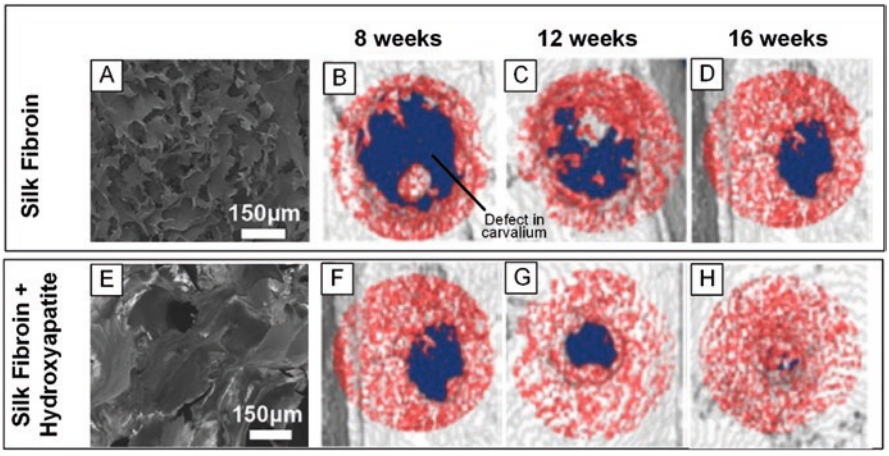

Fig. 3.6 (**a**) SEM images of the structure of (**a**) a silk fibroin hydrogel and (**e**) a silk fibroin–hydroxyapatite composite hydrogel. These hydrogels were injected into a cranial defect within a rat calvarium, and micro-CT images of the skull were used to assess the in vivo bone regeneration (**b** and **f**) 8, (**c** and **g**) 12, and (**d** and **h**) 16 weeks after injection of the hydrogels. (Reproduced from Ding et al. [51])

Gogurla et al. [56] prepared nanocomposites of SF and Au nanoparticles in the form of hydrogels by mixing silk solution and gold(III) chloride trihydrate ($HAuCl_4.3H_2O$) solution at different ratios and aging the mixtures for 15 days at room temperature. They observed negative photoconductive response for the nanocomposites, and they noticed that increasing the concentration of Au nanoparticles enhanced the electrical conductivity and photoconductance yield of the nanocomposites. These novel features of Au-silk nanocomposite hydrogels suggest possible bioelectronic and biophotonic applications such as optical biosensors.

3.3.2 Composite Fibers

SF in the form of electrospun nanofibers possesses high surface-area-to-volume ratio, high porosity, and a wide range of pore size and therefore is a favorable format for cell attachment and proliferation [45]. However, the physical and mechanical properties of electrospun nanofibers from aqueous solutions often need enhancement for practical use in tissue engineering applications. Blending SF with other polymers such as polyethylene oxide [57] and chitosan [58] has been observed to enhance the physical properties of nanofibers. In this regard, Gong et al. [59] pre-

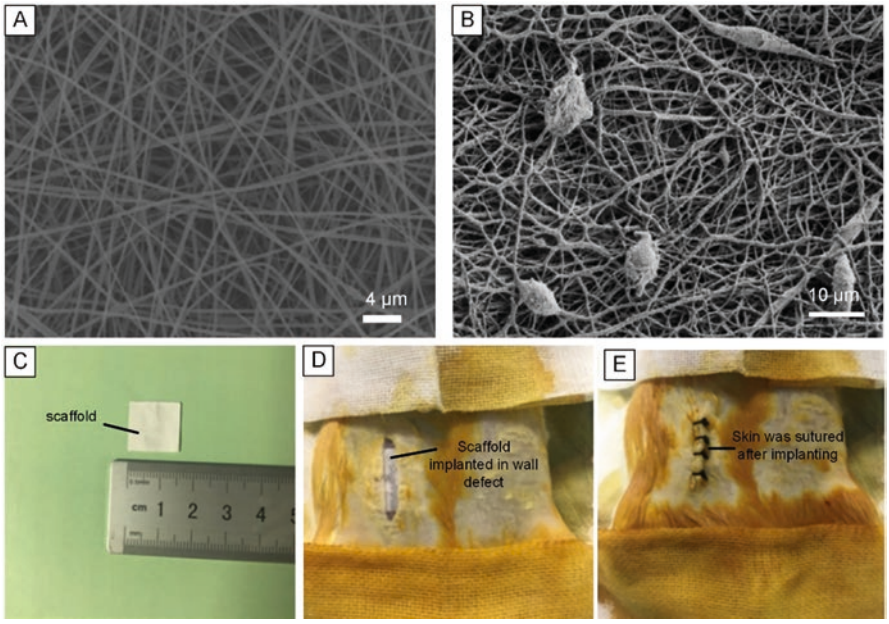

Fig. 3.7 (**a**) SEM image of electrospun composite nanofibers of silk fibroin + poly(3-hydroxybutyrate-co-3-hydroxyvalerate), PHBV, with silk fibroin to PHBV ratio of 75/25. (**b**) FESEM image of HFF-1 fibroblasts cultured on electrospun composite 75/25 nanofibers. (**c**) An electrospun scaffold was prepared by this composition, and (**d**) it was implanted to repair the abdominal wall defect in a rat. (**e**) Then, the skin incision was sutured, and the implant was kept for 15 days. (Reproduced from Gong et al. [59])

pared electrospun nanofibrous scaffolds from blends of SF and poly(3-hydroxybutyrate-co-3-hydroxyvalerate), PHBV, which is a biological polyester. As shown in Fig. 3.7, both in vitro and in vivo experiments were used to evaluate the efficacy of the scaffold in tissue regeneration. Their results showed the effectiveness of the scaffold in abdominal wall defect repair [59].

Apart from blending with other polymers to combine the desired properties of both components, a major approach to improve mechanical properties of RSF fibers is the addition of reinforcing agents such as carbon nanotubes (CNTs) into the spinning dope and making composite mats. Pan et al. [52] added functionalized multiwalled CNTs to RSF solution and fabricated electrospun composite nanofibers. Adding functionalized multiwalled CNTs up to the agglomeration point induced more β-sheet transformation of SF and improved mechanical properties. Furthermore, results indicated biocompatibility for the growth and proliferation of 3T3 cells and Begal's lingua mucosa cells.

3.3.3 Composite Films

In spite of recent advances in modern signal processing techniques, the extensive use of bioelectronic devices still requires applicable materials at the interface of the device and the biological surface [60]. The ever-increasing demand for wearable and flexible bioelectronic devices has led to considerable advances in biopolymers and carbon-based materials [61]. Natural materials such as SF have been investigated in this regard. The fact that SF is nonconductive is advantageous to its application as a dielectric component. However, it eliminates such applications where SF can be used as a direct interface between the device and biological surface, for instance, to control the bioelectrical activity of cells in neuro-regenerative medicine [61]. Therefore, with the aim of expanding the biomedical applications of SF, studies have been done on making composites of silk and conductive nanomaterials such as metallic nanoparticles and CNTs. In this regard, Dionigi et al. [61] used template method to fabricate porous nanostructured conductive films of SF + single-walled CNTs (SWCNTs) composites. Their results showed that the composite film enabled adhesion and differentiation of dorsal root ganglion (DRG) neuron cells in vitro (Fig. 3.8a). In another study, Liu et al. [64] fabricated layered composite films made of an Ag nanowire layer and a silk nanofibril layer using vacuum filtration. Good conductivity and transparency of the composite film made it suitable for designing wearable health-monitoring systems, for example, in cases where a pressure sensor with low detection limit and high response is required.

While making conductive films considerably expands the application of SF films, to meet the requirements of tissue engineering applications, the mechanical performance of RSF films must also be improved. Wang et al. observed that composite films containing SF, glycerol, and low contents of graphene oxide (up to 1%) possessed improved mechanical properties. L-929 fibroblast cells were cultured on these composite films for 7 days. SEM images showed that the cells adhered to the

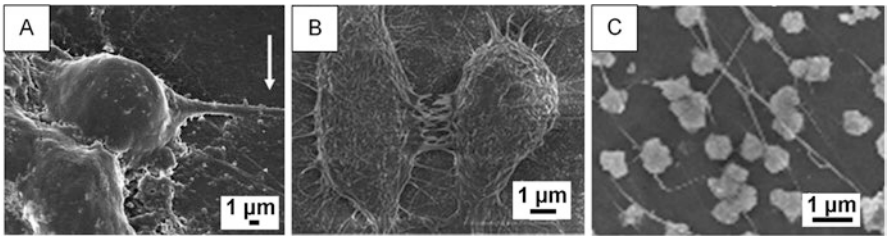

Fig. 3.8 Examples of studies on silk fibroin-based composite films by in vitro cell culturing to assess biocompatibility and cytotoxicity of the composite films. (**a**) Rat DRG neuron cells were grown on a silk fibroin-CNT composite film; SEM image showed the projection from cell body of neurons (white arrow). (**b**) L-929 cells were cultured on silk-graphene oxide composite films. SEM image after 7 days showed that cells tightly adhered to the film and were coated by extracellular matrix. (**c**) Human mesenchymal stem cells (hMSCs) were cultured on silk–silica composite films. SEM image showed mineral deposits on the surface. The mineral nodules come from bone apatite formation, while fibrous structure is due to collagen deposits. (Reproduced from (**a**) Dionigi et al. [61]; (**b**) Wang et al. [62]; (**c**) Mieszawska et al. [63])

films and were covered with extracellular matrix (Fig. 3.8b). Similarly, Mieszawska et al. [63] reported that silica induced good cell viability and proliferation of human mesenchymal stem cells (hMSCs) cultured on the composite films of SF and silica particles. Figure 3.8c shows mineral nodules connected by a collagen-based fibrillar structure after 10 weeks of cell culture on silk-2 μm silica composite films. As another reagent, adding cellulose nanofibrils (CNFs) to regenerated SF is a facile and effective method to improve mechanical properties as well as cell adhesion and proliferation [65].

It is worth noting that a different approach to adding functionality to SF films has been offered by some researchers. Hwang et al. [66] used silk film as the packaging material to seal transient implantable electronic devices which were fabricated on a silk film substrate. Along this line, Min et al. [60] showed that burying a patterned network of randomly connected silver nanowires just beneath the surface of an SF film created a flexible electrode with smooth surface, as a promising alternative for indium tin oxide (ITO) in bioelectronic devices.

In addition to nanowires, carbon nanotubes have been used as additives to SF films along with microwave processing to control the secondary structure of SF films. Cho et al. [17] created RSF–CNT composite films which were then irradiated with microwaves, resulting in local heating and local structural transition of amorphous silk fibroin molecules to stable helical structures. Upon microwave irradiation, a significant increase of helix secondary structure was observed with increasing CNT content. This approach allows a high degree of tailoring the properties and structure of functional regenerated SF-based films for flexible electronics and biomedical devices.

Table 3.4 Comparison of mechanical properties of natural and synthetic fibers used in fiber-reinforced polymer composites [27, 68]

Material	Density (g/cm^3)	Tensile strength (MPa)	Young's modulus (GPa)	Elongation at break (%)
B. mori silk	1.3–1.8	600	6–20	18
Flax	1.3	350–1050	50	3
Hemp	1.48	690	70	1.6
Jute	1.3	400–700	25	1.5
E-glass	2.7	1200	70	2.8
Carbon	1.8	4000	130	2.8

3.3.4 Silk-Fiber-Reinforced Composites

Bio-composites reinforced by natural fibers have been widely studied as potential eco-friendly alternatives to traditional fiber-reinforced composites [67]. On the one hand, traditional reinforcing fibers such as E-glass, flax, and hemp usually have a lower strain at failure and higher stiffness compared with the matrix. On the other hand, as shown in Table 3.4, *B. mori* silk fibers have a relatively low stiffness, about 6–20 GPa, and high strain at failure around 18%. Namely, silk fibers are more ductile compared with traditional polymers such as epoxy and polyester. As a result, silk-fiber-reinforced polymer composites can be described as a ductile fiber and brittle polymer matrix system, in which the toughening mechanism can be fibers acting as crack stoppers.

The technical advantage of silk fibers specific to composite applications is their naturally continuous length and the high compressibility of silk [27]. Silk is the only natural fiber existing as a filament, and thus a high fiber length distribution for effective reinforcing can be achieved by a simple process. Shah et al. [69] studied fiber volume fraction at a compaction pressure of 2.0 bar. Their results revealed that silk was significantly more compactable compared with plant-based fibers and glass fiber. They suggested that silk is suitable for fiber-reinforced composites with high fiber volume fraction.

B. mori silk fibers with a length of 0.5–10 mm were employed as reinforcements for biodegradable polymers such as poly(lactic acid) (PLA), polyurethane, and polybutylene succinate [70–74]. Manjula et al. reported that a small amount of silk fiber (less than 10 wt%) enhanced the mechanical properties and thermal stability of biopolymer. The enhancement was due to good physical interactions between ester-linkage-based biodegradable polymers and silk that consists of various functional groups, assigning polar properties. Zhao et al. prepared silk fiber/PLA bio-composites and reported that water molecules absorbed on silk fiber surface increased the free volume within PLA matrix, facilitating the ester bonds scission during enzymatic degradation measurement. They also concluded that 5 wt% was an optimum content of silk fiber in PLA matrix.

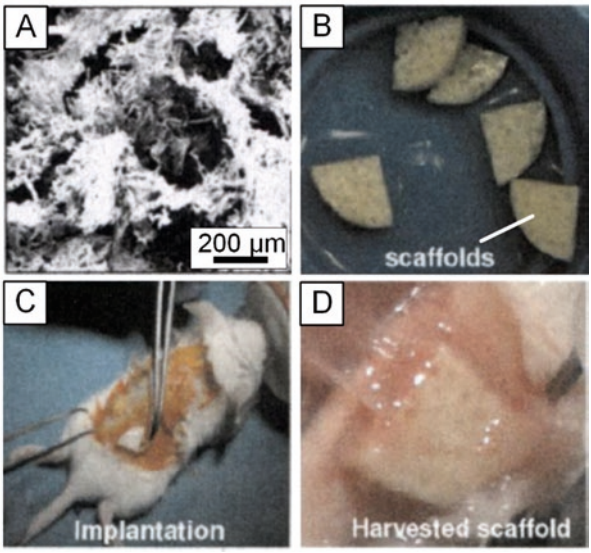

Fig. 3.9 (**a**) SEM image of the structure of a silk-microfiber-reinforced silk porous scaffold. (**b**) Optical photograph of these scaffolds. (**c**) In vivo examination of the scaffolds implanted subcutaneously at the back of mice. After 4 weeks, (**d**) dense tissue ingrowth with vascularization was observed around the implant. (Reproduced from Mandal et al. [75])

In addition to extensive studies on silk-fiber-reinforced polymers, a newer approach has been to fabricate silk-fiber-reinforced SF matrix [53]. Among natural hydrogel materials, tunable degradability of SF makes it excellent for in vivo applications [53]. Additionally, strong interfacial bonding between the two silk phases is beneficial for mechanical properties as the contribution of fibers to matrix reinforcement depends on the strength of interfacial bonding between the two. However, improving mechanical properties of SF hydrogels through fiber reinforcement requires knowledge on tissue development behavior of the composite system. Therefore, Mandal et al. [75] fabricated SF microfiber-reinforced SF hydrogels and implanted them into the back of some mice. After 4 weeks, they observed that the retrieved implants were surrounded by a dense tissue and that the implants and mice tissue were closely integrated (Fig. 3.9).

3.3.5 Hybrid Nanocomposites

As the basic architectural component of SF, silk nanofibrils (SNFs) can be grown and assembled from regenerated SF solution. Novel hybrids can be made by mixing functional nanomaterials such as silver nanowires or nanohydroxyapatite with SNFs [64, 76]. Liu et al. [64] performed vacuum filtration on a mixture of SNFs and Ag nanowire solutions to fabricate hybrid films with humidity-sensitive conductivity in various shapes. This feature along with good biocompatibility and skin affinity of

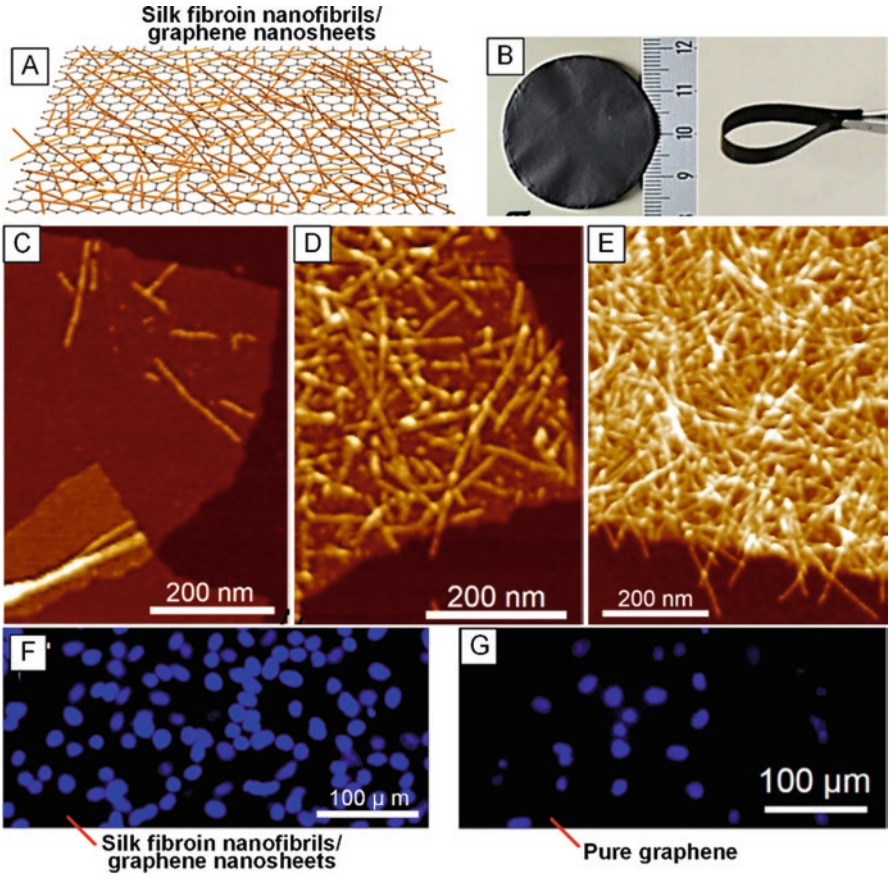

Fig. 3.10 (**a**) Schematic representation of silk nanofibrils growth on graphene nanosheets, which is formed under certain conditions of mass ratio and pH. (**b**) A composite film made by vacuum filtration of the solution mixture. The effect of mass ratio of silk nanofibers to graphene nanosheets on the hybrids was revealed by AFM at pH = 10.3. Nanofibril/graphene mass ratios were (**c**) 3/7, (**d**) 5/5, and (**e**) 8/2. The growth of stained Hela cells on the surface of hybrid film was monitored for 3 days. (**f**) The fluorescent area of the 8/2 hybrid film was about five times larger than (**g**) that for pure graphene, showing better cell adhesion and growth for hybrids. (Reproduced from Ling et al. [77])

SNFs make these hybrid films suitable for wearable health monitoring devices. Ling et al. [77] grew SNFs on graphene nanosheets (Fig. 3.10a) under different processing conditions (Fig. 3.10c–e) and fabricated nanocomposite films (Fig. 3.10b) with different ratios between SNFs and graphene nanosheets. Along with other physical and mechanical properties, they evaluated cell adhesion and proliferation of Hela cells. The film with SNF to graphene ratio of 8:2 showed better cell growth compared with a pure graphene film after 3 days of cell culture (Fig. 3.10f and g).

3.3.6 *Carbonized Silk*

SF as a carbon precursor has been reported recently [11, 78–80]. Generally, β-sheet-rich proteins such as silk protein can be transformed into hexagonal carbon structure through a simple thermal treatment under an inert atmosphere. Upon heating silk protein from 250 °C (the onset of thermal degradation) to 2800 °C, major chemical change and dramatic increase in conductivity occur between 300 °C and 350 °C. The carbonization of silk fibers at 800 °C was investigated, and pseudo-graphitic carbon was obtained with a carbon yield of 30% which is a higher yield than cellulose-based carbon. Further heating will result in a more developed graphitic structure. Both native silkworm silk fiber and RSF materials transform into carbon materials by heat treatment under inert atmosphere without stabilization step in air [11]. Good performance of carbonized silkworm cocoon and RSF has been reported in energy storage and conversion applications.

Flexible wearable strain sensors and skin-like pressure sensors with an electrically conductive sensing element such as metal- or carbon-nanomaterials and a flexible substrate have drawn great interest. The main challenges include finding cost-effective and environmentally friendly ways of fabricating sensors with both high sensitivity and a broad range of sensing [54, 81, 82]. Carbon materials derived

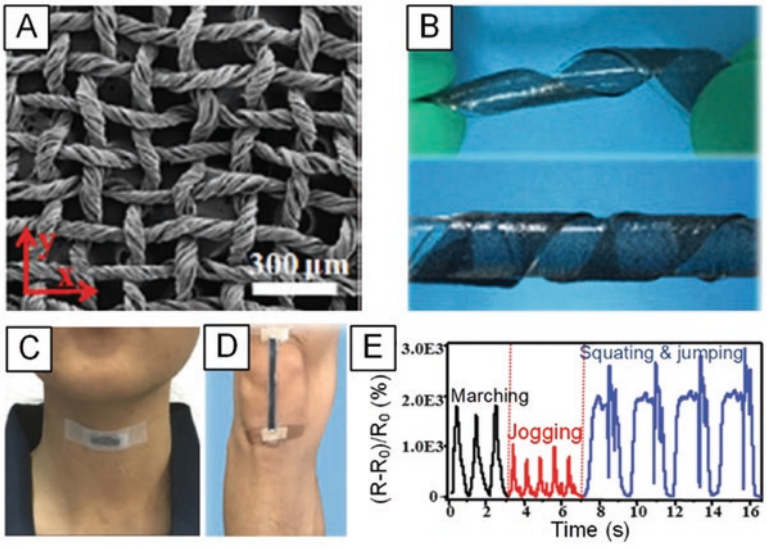

Fig. 3.11 (**a**) The SEM image of a carbonized silk fabric used to make (**b**) highly flexible strain sensors with high sensitivity and strain range. These sensors can be attached to different parts of the body, for example, (**c**) the throat or (**d**) the knee joint, to detect wide range of human activities. Different movements of the knee joint can be tracked by (**e**) recording the relative change in the resistance of the sensor over time. (Reproduced from (**a**, **b**, **d**, **e**) Wang et al. [81]; (**c**) Wang et al. [54])

from biomaterials such as silk have interesting features to be utilized in electronic devices. Unlike CNTs and graphene, carbon materials derived from biomaterials have the requirements to overcome the abovementioned challenges. Wang et al. [54, 81] made wearable strain sensors based on carbonized silk fabric and showed that the woven structure of silk fabric was well reserved after carbonization (Fig. 3.11a). Bulk shape stability had previously been reported by Liang et al. [78] during carbonization of silk cocoon. Wang et al. [54, 81] reported the influence of the woven structure of initial silk fabric on the performance of the sensor such as its sensitivity, response time, and detection limit. Figure 3.11b shows a strain sensor made by encapsulating the carbonized silk fabric within PDMS. These sensors are capable of detecting a wide range of human motions from subtle muscle movements during speech (Fig. 3.11c) to vigorous movements of knee joint (Fig. 3.11d). The sensor can differentiate various movements of the knee joint based on the relative change in the resistance of the sensor (Fig. 3.11e). Carbonized silk nanofiber membrane has also been utilized in pressure sensors. Wang et al. [82] investigated the performance of the sensors based on varying the electrospinning time during the preparation of silk nanofiber membranes, which resulted in carbonized silk nanofiber membranes with various thicknesses. The sensors made from thinner membranes showed higher sensitivities.

3.4 Summary and Outlook

Considerations regarding sustainable and environmentally friendly production have led to substantial developments in new manufacturing techniques to utilize natural materials, especially for biomedical applications. In this regard, silk fibroin from *B. mori* silkworm has been considered as a promising material due to their abundance, remarkable mechanical properties, and the facile processing techniques associated with controlling both its macroscopic form and micro-to-nanoscale morphology. At the heart of these simple processing techniques lies the RSF solution that makes silk material formats so diverse. For biomedical applications, however, more restrictions are applied on the chemical solvents and additives that can be used during processing of silk. While SF-based materials have opened several opportunities in biomedical field, considerable amount of research has also been dedicated to finding new approaches to adding functionality while maintaining its remarkable biocompatibility and tunable biodegradability. Interestingly, these approaches are quite similar regardless of the material format. In this chapter, we explain traditional mixing of SF with a secondary phase to make silk-derived composites in the form of hydrogels, fibers, and films. Then, we point at a more recent approach to grow and assemble silk nanofibrils from RSF solution and exploit them in novel nanocomposites. While the studies reviewed in this section deal with formation of silk nanofibrils, there are recent studies that try to obtain other stable building blocks such as silk nanoribbons through a proper choice of solvent system. Therefore, a potential future research direction can be aimed at the development of hybrid

nanocomposites based on silk nanoribbons and other controlled morphologies. Finally, we introduce carbonized silk protein with the capability of rendering silk electrically conductive, while preserving its original form. While research on carbonized silk cocoon/fibroin continues, review of recent literature reveals that some researchers are looking at the carbonization of silk coated with nanoparticles or some polymers such as polypyrrole. In summary, research on silk fiber has been growing fast, and there is more room to be explored in this area in order to realize many biomedical technologies.

References

1. G. Chen, J. Guan, T. Xing, X. Zhou, Properties of silk fibers modified with diethylene glycol dimethacrylate. J. Appl. Polym. Sci. **102**, 424–428 (2006). https://doi.org/10.1002/app.24064
2. J.G. Hardy, L.M. Römer, T.R. Scheibel, Polymeric materials based on silk proteins. Polymer (Guildf) **49**, 4309–4327 (2008). https://doi.org/10.1016/j.polymer.2008.08.006
3. B. Kundu, R. Rajkhowa, S.C. Kundu, X. Wang, Silk fibroin biomaterials for tissue regenerations. Adv. Drug Deliv. Rev. **65**, 457–470 (2013). https://doi.org/10.1016/j.addr.2012.09.043
4. H.J. Jin, D.L. Kaplan, Mechanism of silk processing in insects and spiders. Nature **424**, 1057–1061 (2003). https://doi.org/10.1038/nature01809
5. S. Keten, Z. Xu, B. Ihle, M.J. Buehler, Nanoconfinement controls stiffness, strength and mechanical toughness of B-sheet crystals in silk. Nat. Mater. **9**, 359–367 (2010). https://doi.org/10.1038/nmat2704
6. F.G. Omenetto, New opportunities for an ancient material. Science **329**, 528–531 (2011). https://doi.org/10.1126/science.1188936
7. G.R. Plaza, P. Corsini, E. Marsano, et al., Old silks endowed with new properties. Macromolecules **42**, 8977–8982 (2009). https://doi.org/10.1021/ma9017235
8. S. Ling, Z. Qin, C. Li, et al., Polymorphic regenerated silk fibers assembled through bioinspired spinning. Nat. Commun. **8**, 1387 (2017). https://doi.org/10.1038/s41467-017-00613-5
9. F. Teule, Y.-G. Miao, B.-H. Sohn, et al., Silkworms transformed with chimeric silkworm/spider silk genes spin composite silk fibers with improved mechanical properties. Proc. Natl. Acad. Sci. **109**, 923–928 (2012). https://doi.org/10.1073/pnas.1109420109
10. G. Zhou, Z. Shao, D.P. Knight, et al., Silk fibers extruded artificially from aqueous solutions of regenerated bombyx mori silk fibroin are tougher than their natural counterparts. Adv. Mater. **21**, 366–370 (2009). https://doi.org/10.1002/adma.200800582
11. S.Y. Cho, Y.S. Yun, S. Lee, et al., Carbonization of a stable β-sheet-rich silk protein into a pseudographitic pyroprotein. Nat. Commun. **6**, 7145–7151 (2015). https://doi.org/10.1038/ncomms8145
12. T. Asakura, R. Sugino, T. Okumura, Y. Nakazawa, The role of irregular unit, GAAS, on the secondary structure of Bombyx mori silk fibroin studied with 13C CP/MAS NMR and wide-angle X-ray scattering. Protein Sci. **11**, 1873–1877 (2002). https://doi.org/10.1110/ps.0208502
13. S. Inoue, K. Tanaka, F. Arisaka, et al., Silk fibroin of Bombyx mori is secreted, assembling a high molecular mass elementary unit consisting of H-chain, L-chain, and P25, with a 6:6:1 molar ratio. J. Biol. Chem. **275**, 40517–40528 (2000). https://doi.org/10.1074/jbc.M006897200
14. M. Chevillard, P. Couble, J.-C. Prudhomme, Complete nucleotide sequence of the gene encoding the Bombyx mori silk protein P25 and predicted amino acid sequence of the protein. Nucleic Acids Res. **14**, 6341–6342 (1986)
15. K. Tanaka, S. Inoue, S. Mizuno, Hydrophobic interaction of P25, containing Asn-linked oligosaccharide chains, with the H-L complex of silk fibroin produced by Bombyx mori. Insect Biochem. Mol. Biol. **29**, 269–276 (1999). https://doi.org/10.1016/S0965-1748(98)00135-0

16. A.R. Murphy, D.L. Kaplan, Biomedical applications of chemically-modified silk fibroin. J. Mater. Chem. **19**, 6443–6450 (2009). https://doi.org/10.1039/b905802h
17. S.Y. Cho, M. Abdulhafez, M.E. Lee, et al., Promoting Helix-Rich Structure in Silk Fibroin Films through Molecular Interactions with Carbon Nanotubes and Selective Heating for Transparent Biodegradable Devices. ACS Appl Nano Mater acsanm **1**, 5441–5450 (2018). https://doi.org/10.1021/acsanm.8b00784
18. C. Vepari, D.L. Kaplan, Silk as a biomaterial. Prog. Polym. Sci. **32**, 991–1007 (2007). https://doi.org/10.1016/j.progpolymsci.2007.05.013
19. C.Z. Zhou, F. Confalonieri, M. Jacquet, et al., Silk fibroin: Structural implications of a remarkable amino acid sequence. Proteins Struct. Funct. Genet. **44**, 119–122 (2001). https://doi.org/10.1002/prot.1078
20. L.F. Drummy, B.L. Farmer, R.R. Naik, Correlation of the β-sheet crystal size in silk fibers with the protein amino acid sequence. Soft Matter **3**, 877–882 (2007). https://doi.org/10.1039/B701220A
21. J. Guan, D. Porter, F. Vollrath, Thermally induced changes in dynamic mechanical properties of native silks. Biomacromolecules **14**, 930–937 (2013). https://doi.org/10.1021/bm400012k
22. X. Hu, D. Kaplan, P. Cebe, Effect of water on the thermal properties of silk fibroin. Thermochim. Acta **461**, 137–144 (2007). https://doi.org/10.1016/j.tca.2006.12.011
23. J. Pérez-Rigueiro, C. Viney, J. Llorca, M. Elices, Mechanical properties of single-brin silkworm silk. J. Appl. Polym. Sci. **75**, 1270–1277 (2000). https://doi.org/10.1002/(SICI)1097-4628(20000307)75:10<1270::AID-APP8>3.0.CO;2-C
24. C. Viney, J. Llorca, M. Elices, J. Pe, Silkworm silk as an engineering material. J. Appl. Polym. Sci. **70**, 2439–2447 (1998). https://doi.org/10.1002/(SICI)1097-4628(19981219)70:12<2439::AID-APP16>3.0.CO;2-J
25. T.B. Lewis, L.E. Nielsen, Dynamic mechanical properties of particulate-filled composites. J. Appl. Polym. Sci. **14**, 1449–1471 (1970). https://doi.org/10.1002/app.1970.070140604
26. D. Porter, F. Vollrath, K. Tian, et al., A kinetic model for thermal degradation in polymers with specific application to proteins. Polymer (Guildf) **50**, 1814–1818 (2009). https://doi.org/10.1016/j.polymer.2009.01.064
27. D.U. Shah, D. Porter, F. Vollrath, Can silk become an effective reinforcing fibre? A property comparison with flax and glass reinforced composites. Compos. Sci. Technol. **101**, 173–183 (2014). https://doi.org/10.1016/j.compscitech.2014.07.015
28. D.N. Rockwood, R.C. Preda, T. Yücel, et al., Materials fabrication from Bombyx mori silk fibroin. Nat. Protoc. **6**, 1612–1631 (2011). https://doi.org/10.1038/nprot.2011.379
29. L. Meinel, S. Hofmann, V. Karageorgiou, et al., The inflammatory responses to silk films in vitro and in vivo. Biomaterials **26**, 147–155 (2005). https://doi.org/10.1016/j.biomaterials.2004.02.047
30. L.S. Wray, X. Hu, J. Gallego, et al., Effect of processing on silk-based biomaterials: Reproducibility and biocompatibility. J. Biomed. Mater. Res.Part B Appl. Biomater. **99**(B), 89–101 (2011). https://doi.org/10.1002/jbm.b.31875
31. N. Sasithorn, L. Martinová, Fabrication of Silk Nanofibres with Needle and Roller Electrospinning Methods. J. Nanomater. **2014**, 1–9 (2014). https://doi.org/10.1155/2014/947315
32. Y. Tamada, New process to form a silk fibroin porous 3-D structure. Biomacromolecules **6**, 3100–3106 (2005). https://doi.org/10.1021/bm050431f
33. J. Qu, L. Wang, Y. Hu, et al., Preparation of Silk Fibroin Microspheres and Its Cytocompatibility. J. Biomater. Nanobiotechnol. **4**, 84–90 (2013). 10.4028. https://doi.org/10.4236/jbnb.2013.41011
34. U.J. Kim, J. Park, C. Li, et al., Structure and properties of silk hydrogels. Biomacromolecules **5**, 786–792 (2004). https://doi.org/10.1021/bm0345460
35. M.L. Lovett, C.M. Cannizzaro, G. Vunjak-Novakovic, D.L. Kaplan, Gel spinning of silk tubes for tissue engineering. Biomaterials **29**, 4650–4657 (2008). https://doi.org/10.1016/j.biomaterials.2008.08.025

36. L.D. Koh, Y. Cheng, C.P. Teng, et al., Structures, mechanical properties and applications of silk fibroin materials. Prog. Polym. Sci. **46**, 86–110 (2015). https://doi.org/10.1016/j.progpolymsci.2015.02.001
37. C. Fu, Z. Shao, V. Fritz, Animal silks: Their structures, properties and artificial production. Chem. Commun. 6515–6529 (2009). https://doi.org/10.1039/b911049f
38. I.C. Um, H. Kweon, Y.H. Park, S. Hudson, Structural characteristics and properties of the regenerated silk fibroin prepared from formic acid. Int. J. Biol. Macromol. **29**, 91–97 (2001). https://doi.org/10.1016/S0141-8130(01)00159-3
39. L.F. Drummy, D.M. Phillips, M.O. Stone, et al., Thermally induced alpha-helix to beta-sheet transition in regenerated silk fibers and films. Biomacromolecules **6**, 3328–3333 (2005). https://doi.org/10.1021/bm0503524
40. S. Lu, X. Wang, Q. Lu, et al., Insoluble and flexible silk films containing glycerol. Biomacromolecules **11**, 143–150 (2010b). https://doi.org/10.1021/bm900993n
41. Q. Lu, X. Hu, X. Wang, et al., Water-insoluble silk films with silk I structure. Acta Biomater. **6**, 1380–1387 (2010a). https://doi.org/10.1016/j.actbio.2009.10.041
42. O.N. Tretinnikov, Y. Tamada, Influence of casting temperature on the near-surface structure and wettability of cast silk fibroin films. Langmuir **17**, 7406–7413 (2001). https://doi.org/10.1021/la010791y
43. H.J. Jin, J. Park, V. Karageorgiou, et al., Water-stable silk films with reduced β-sheet content. Adv. Funct. Mater. **15**, 1241–1247 (2005). https://doi.org/10.1002/adfm.200400405
44. X. Hu, K. Shmelev, L. Sun, et al., Regulation of silk material structure by temperature-controlled water vapor annealing. Biomacromolecules **12**, 1686–1696 (2011). https://doi.org/10.1021/bm200062a
45. K.H. Kim, L. Jeong, H.N. Park, et al., Biological efficacy of silk fibroin nanofiber membranes for guided bone regeneration. J. Biotechnol. **120**, 327–339 (2005). https://doi.org/10.1016/j.jbiotec.2005.06.033
46. Z. Chen, N. Zhong, J. Wen, et al., Porous Three-Dimensional Silk Fibroin Scaffolds for Tracheal Epithelial Regeneration in Vitro and in Vivo. ACS Biomater. Sci. Eng. **4**, 2977–2985 (2018). https://doi.org/10.1021/acsbiomaterials.8b00419
47. T.K. Mwangi, R.D. Bowles, D.M. Tainter, et al., Synthesis and characterization of silk fibroin microparticles for intra-articular drug delivery. Int. J. Pharm. **485**, 7–14 (2015). https://doi.org/10.1016/j.ijpharm.2015.02.059
48. M. Farokhi, F. Mottaghitalab, Y. Fatahi, et al., Overview of Silk Fibroin Use in Wound Dressings. Trends Biotechnol. **36**, 907–922 (2018). https://doi.org/10.1016/j.tibtech.2018.04.004
49. S. Enomoto, M. Sumi, K. Kajimoto, et al., Long-term patency of small-diameter vascular graft made from fibroin, a silk-based biodegradable material. J. Vasc. Surg. **51**, 155–164 (2009). https://doi.org/10.1016/j.jvs.2009.09.005
50. W. Zhang, L. Chen, J. Chen, et al., Silk Fibroin Biomaterial Shows Safe and Effective Wound Healing in Animal Models and a Randomized Controlled Clinical Trial. Adv. Healthc. Mater. **6**, 1700121 (2017). https://doi.org/10.1002/adhm.20170012
51. Z. Ding, H. Han, Z. Fan, et al., Nanoscale silk-hydroxyapatite hydrogels for injectable bone biomaterials. ACS Appl. Mater. Interfaces **9**, 16913–16921 (2017). https://doi.org/10.1021/acsami.7b03932
52. H. Pan, Y. Zhang, Y. Hang, et al., Significantly reinforced composite Fibers electrospun from silk fibroin/carbon nanotube aqueous solutions. Biomacromolecules **13**, 2859–2867 (2012). https://doi.org/10.1021/bm300877d
53. S. Yodmuang, B.B. Mandal, S.L. McNamara, et al., Silk microfiber-reinforced silk hydrogel composites for functional cartilage tissue repair. Acta Biomater. **11**, 27–36 (2014). https://doi.org/10.1016/j.actbio.2014.09.032
54. C. Wang, X. Li, E. Gao, et al., Carbonized silk fabric for ultrastretchable, highly sensitive, and wearable strain sensors. Adv. Mater. **28**, 6640–6648 (2016). https://doi.org/10.1002/adma.201601572
55. D.A. Frauchiger, A. Tekari, M. Wöltje, et al., A review of the application of reinforced hydrogels and silk as biomaterials for intervertebral disc repair. Eur. Cell. Mater. **34**, 271–290 (2017). https://doi.org/10.22203/eCM.v034a17

56. N. Gogurla, A.K. Sinha, D. Naskar, et al., Metal nanoparticles triggered persistent negative photoconductivity in silk protein hydrogels. Nanoscale **8**, 7695–7703 (2016). https://doi.org/10.1039/C6NR01494A
57. H.J. Jin, S.V. Fridrikh, G.C. Rutledge, D.L. Kaplan, Electrospinning Bombyx mori silk with poly(ethylene oxide). Biomacromolecules **3**, 1233–1239 (2002). https://doi.org/10.1021/bm025581u
58. W.H. Park, L. Jeong, Y.D. Il, S. Hudson, Effect of chitosan on morphology and conformation of electrospun silk fibroin nanofibers. Polymer (Guildf) **45**, 7151–7157 (2004). https://doi.org/10.1016/j.polymer.2004.08.045
59. W. Gong, T. Cheng, Q. Liu, et al., Surgical repair of abdominal wall defect with biomimetic nano/microfibrous hybrid scaffold. Mater. Sci. Eng. C **93**, 828–837 (2018). https://doi.org/10.1016/j.msec.2018.08.053
60. K. Min, M. Umar, H. Seo, et al., Biocompatible, optically transparent, patterned, and flexible electrodes and radio-frequency antennas prepared from silk protein and silver nanowire networks. RSC Adv. **7**, 574–580 (2017). https://doi.org/10.1039/C6RA25580A
61. C. Dionigi, T. Posati, V. Benfenati, et al., A nanostructured conductive bio-composite of silk fibroin–single walled carbon nanotubes. J. Mater. Chem. B **2**, 1424 (2014). https://doi.org/10.1039/c3tb21172j
62. L. Wang, C. Lu, B. Zhang, et al., Fabrication and characterization of flexible silk fibroin films reinforced with graphene oxide for biomedical applications. RSC Adv. **4**, 40312–40320 (2014). https://doi.org/10.1039/c4ra04529g
63. A.J. Mieszawska, N. Fourligas, I. Georgakoudi, et al., Osteoinductive silk-silica composite biomaterials for bone regeneration. Biomaterials **31**, 8902–8910 (2010). https://doi.org/10.1016/j.biomaterials.2010.07.109
64. J. Liu, T. He, G. Fang, et al., Environmentally responsive composite films fabricated using silk nanofibrils and silver nanowires. J. Mater. Chem. C **6**, 12940–12947 (2018). https://doi.org/10.4236/10.1039/C8TC04549F
65. Y. Feng, X. Li, M. Li, et al., Facile preparation of biocompatible silk fibroin/cellulose nanocomposite films with high mechanical performance. ACS Sustain. Chem. Eng. **5**, 6227–6236 (2017). https://doi.org/10.1021/acssuschemeng.7b01161
66. S-W. Hwang, H. Tao, D-H. Kim, et al., A physically transient form of silicon electronics. Science (80-) **337**, 1640–1645 (2012). https://science.sciencemag.org/content/337/6102/1640
67. O. Faruk, A.K. Bledzki, H.P. Fink, M. Sain, Biocomposites reinforced with natural fibers: 2000-2010. Prog. Polym. Sci. **37**, 1552–1596 (2012). https://doi.org/10.1016/j.progpolymsci.2012.04.003
68. A.U. Ude, R.A. Eshkoor, R. Zulkifili, et al., Bombyx mori silk fibre and its composite: A review of contemporary developments. Mater. Des. **57**, 298–305 (2014). https://doi.org/10.1016/j.matdes.2013.12.052
69. D.U. Shah, Developing plant fibre composites for structural applications by optimising composite parameters: A critical review. J. Mater. Sci. **48**, 6083–6107 (2013). https://doi.org/10.1007/s10853-013-7458-7
70. H.Y. Cheung, K.T. Lau, Y.F. Pow, et al., Biodegradation of a silkworm silk/PLA composite. Compos. Part B Eng. **41**, 223–228 (2010). https://doi.org/10.1016/j.compositesb.2009.09.004
71. S.O. Han, H.J. Ahn, D. Cho, Hygrothermal effect on henequen or silk fiber reinforced poly(butylene succinate) biocomposites. Compos. Part B Eng. **41**, 491–497 (2010). https://doi.org/10.1016/j.compositesb.2010.05.003
72. M.P. Ho, K.T. Lau, H. Wang, D. Bhattacharyya, Characteristics of a silk fibre reinforced biodegradable plastic. Compos. Part B Eng. **42**, 117–122 (2011). https://doi.org/10.1016/j.compositesb.2010.10.007
73. M. Takeda, M. Ikeda, S. Satoh, et al., Rab13 is involved in the entry step of hepatitis C virus infection. Acta Med. Okayama **70**, 111–118 (2016). https://doi.org/10.1002/pen
74. Y.Q. Zhao, H.Y. Cheung, K.T. Lau, et al., Silkworm silk/poly(lactic acid) biocomposites: Dynamic mechanical, thermal and biodegradable properties. Polym. Degrad. Stab. **95**, 1978–1987 (2010). https://doi.org/10.1016/j.polymdegradstab.2010.07.015

75. B.B. Mandal, A. Grinberg, E.S. Gil, et al., High-sltrength silk protein scaffolds for bone repair. Proc. Natl. Acad. Sci. U. S. A. **109**, 7699–7704 (2012). https://doi.org/10.1073/pnas.1
76. R. Mi, Y. Liu, X. Chen, Z. Shao, Structure and properties of various hybrids fabricated by silk nanofibrils and nanohydroxyapatite. Nanoscale **8**, 20096–20102 (2016). https://doi.org/10.1039/c6nr07359j
77. S. Ling, C. Li, J. Adamcik, et al., Directed growth of silk nanofibrils on graphene and their hybrid nanocomposites. ACS Macro Lett. **3**, 146–152 (2014). https://doi.org/10.1021/mz400639y
78. Y. Liang, D. Wu, R. Fu, Carbon microfibers with hierarchical porous structure from electrospun fiber-like natural biopolymer. Sci. Rep. **3**, 1–5 (2013). https://doi.org/10.1038/srep01119
79. M. Majibur Rahman Khan, Y. Gotoh, H. Morikawa, M. Miura, Graphitization behavior of iodine-treated Bombyx mori silk fibroin fiber. J. Mater. Sci. **44**, 4235–4240 (2009). https://doi.org/10.1007/s10853-009-3557-x
80. Y.S. Yun, S.Y. Cho, J. Shim, et al., Microporous carbon nanoplates from regenerated silk proteins for supercapacitors. Adv. Mater. **25**, 1993 (2013). https://doi.org/10.1002/adma.201204692
81. C. Wang, K. Xia, M. Jian, et al., Carbonized silk georgette as an ultrasensitive wearable strain sensor for full-range human activity monitoring. J. Mater. Chem. C **5**, 7604–7611 (2017a). https://doi.org/10.1039/c7tc01962a
82. Q. Wang, M. Jian, C. Wang, Y. Zhang, Carbonized silk nanofiber membrane for transparent and sensitive electronic skin. Adv. Funct. Mater. **27**, 1605657 (2017b). https://doi.org/10.1002/adfm.201605657